

Citation: Sinki, K., Y. Fujii, B. Shibazaki (2021), Numerical simulations of the 1992 Flores tsunami using earthquake fault and landslide models, Synopsis of IISEE-GRIPS Master's Thesis.

# NUMERICAL SIMULATIONS OF THE 1992 FLORES TSUNAMI USING EARTHQUAKE FAULT AND LANDSLIDE MODELS

Kian Purna Sinki<sup>1,2</sup>

Supervisor: Yushiro FUJII<sup>3</sup>, Bunichiro SHIBAZAKI<sup>3</sup>

## ABSTRACT

The Flores back-arc thrust is an active earthquake source in northern Flores Island, and this trench extends from Bali to East Flores. On December 12, 1992, there was an earthquake that caused a massive tsunami. The tsunami that hit along the northern coast of Flores caused many economic and infrastructure damages and loss of life. The field survey measurements indicate that the highest tsunami was 26 m in northern coast of the Flores, revealing significantly high tsunami run-ups which might be caused by landslides because there were some evidences of landslide slumps in several areas.

This study reproduces the tsunami propagation and inundation for the 1992 Flores tsunami and compares the numerical results with the observed data obtained by the field survey. We applied the numerical simulation using a finite difference TUNAMI code that solves the non-linear shallow water equations. We used BATNAS bathymetric data and DEMNAS topographic data, which were provided by Indonesia Geospatial Agency for two-layer computations to simulate tsunamis from the fault models and three-layer computations for fault and landslide models. We also propose a scenario earthquake for creating a tsunami hazard map with a reference fault model from the previous study.

Using the data we collected, we have successfully performed the tsunami modeling for wave propagation to the northern coast of Flores. The simulated tsunami by using the three-layer computations with the fault and landslide models generated higher tsunamis than the two-layer computations only with the fault models. It is emphasized that the landslide will impact the tsunami generation higher than the fault only. Besides, we also obtained the maximum tsunami run-up heights and inundation distances. This study will bring many advantages to enhance the source input for tsunami simulations since we found that the results are applicable to create the tsunami hazard map in the Flores area.

**Keywords:** 1992 Flores Earthquake and Tsunami, Earthquake Fault and Landslide Model, Tsunami Hazard Map.

## 1. INTRODUCTION

Indonesia is located between the Pacific Ocean and the Indian Ocean and lies on the boundaries of major tectonic plates: the Indo-Australian Plate that subducts beneath the Eurasian Plate (Sunda Plate), the Pacific Plate in the eastern part, Philippine Sea Plate in the northeastern part (Hamilton, 1979). Flores Island located in the Eastern Nusa Tenggara, a seismically active area. In 1992, the earthquake of Mw

---

<sup>1</sup> Agency for Meteorology, Climatology and Geophysics (BMKG), Jakarta, Indonesia.

<sup>2</sup> IISEE-GRIPS Master's course student.

<sup>3</sup> International Institute of Seismology and Earthquake Engineering (IISEE), Building Research Institute (BRI).

7.2 caused the devastating tsunami (Figure 1). The fault extended from the north of the Flores Island to the north-sea of Bali with a length around 1,130 km and located between the subduction boundary of the Indo-Australian and Eurasian plates (Daryono, 2011). Tsuji et al. (1995) reported that the people felt the great shaking at Maumere in Wuring city with the maximum intensity recorded up to VII MMI. This tsunami caused catastrophic damage along the coast of northeast Flores, based on the field survey along coastal parts of the Flores Island, they found the highest tsunami run-up with the average of 18 m in the most northeast shore. Yeh et al. (1993) found some evidences of landslides along the southern coast of Hading Bay, the eastern part of Flores, which may have caused the extremely high tsunami run-ups. In order to contribute to a better quantitative understanding of the tsunami propagation and inundation around Flores, as well as those for the 1992 Flores tsunami we adopt some earthquake fault and landslide models. We will evaluate the simulated tsunami by comparing with the field survey data by Tsuji et al. (1995) and also create a tsunami hazard map of the western part of Flores Island assuming an earthquake scenario model.

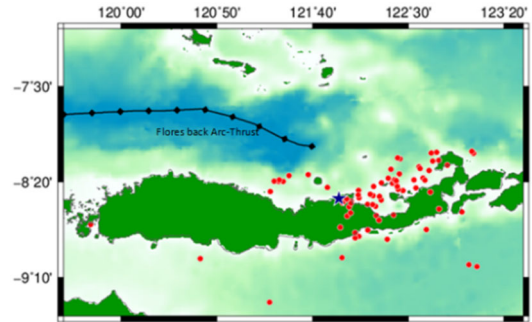


Figure 1. Epicenter (blue star) of the 1992 Flores earthquake and the aftershocks (red circles) distribution from USGS.

## 2. DATA

### 2.1 Tectonic source – Earthquake’s fault models

Imamura et al. (1995) and Pranantyo and Cummins (2019) constructed the different fault models for this earthquake as shown in Figure 2. Imamura et al. (1995) proposed a two-fault model and we modified their parameters as listed in Table 1. Pranantyo and Cummins (2019) constructed the subfault model by the finite-fault source inversion using the seismic data, which can be used for tsunami simulations. The inverted slip model have 360 subfaults to obtain the heterogeneous slips on the fault. The maximum slip on the fault is about 20 m, and large slips focused on the western part near the hypocenter.

Table 1. Parameters of fault model modified from Imamura et al.

Subfault	Longitude (deg)	Latitude (deg)	Length (km)	Width (km)	Depth (km)	Strike (deg)	Dip (deg)	Rake (deg)	Slip (m)	Mw
West	121.93	-8.46	52	27	3	65	32	64	3.2	7.7
East	122.3578	-8.262585	52	27	3	65	32	64	9.6	7.9

### 2.2. Field survey data

As the observed data in this study, we referred to Hidayat et al. (1995). They conducted tsunami modeling in 37 locations by compiling the tsunami run-up heights (Figure 3) from the field survey results from Tsuji et al. (1995). The tsunami field survey was conducted along the northeast shore of Flores Island. The yellow number indicates the tsunami run-up heights and the green numbers shows the location of the field survey measurement. For this study we will discuss the results for Wuring (11), Maumere (12), Babi Island (25) and (27) Uepadung (33), Waibalen (34), Pantai Lela (35), Riangkroko (36) and Bunga (37).

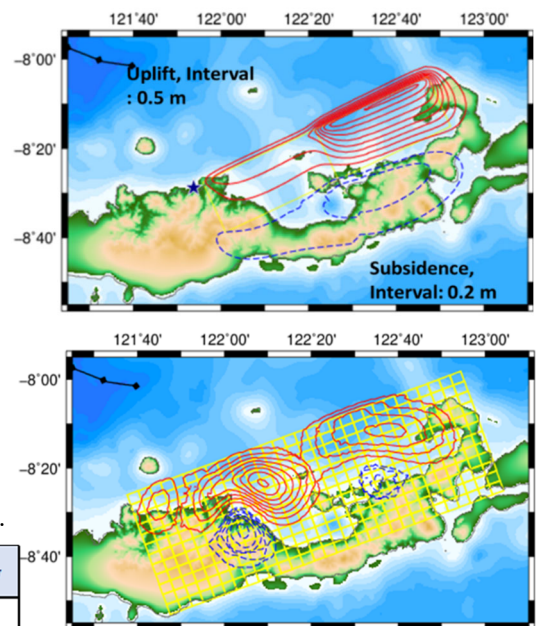


Figure 2. Fault models form (top) Imamura et al. (1995) and (bottom) Pranantyo and Cummins (2019), and the calculated seafloor deformations.

### 2.3. Nontectonic source – Landslide models

Based on the information reported by Tsuji et al (1995) and Yeh et al. (1993), we adopted the slump-type submarine landslide model by Watts et al. (2005). Figure 4 shows the calculated sea surface elevations from the constructed three landslide models. The first landslide model near Waibalen has the maximum uplift of 18.7 m and subsidence of -21.0 m. For the second model near Riangkroko, the maximum uplift is 18.3 m and the subsidence is -20.6 m, and for the third model near Bunga the value of the maximum uplift is 20.1 m and the subsidence value is -21 m. The uplift and subsidence information are considered as the bathymetry and topography deformation for the initial tsunami wave.

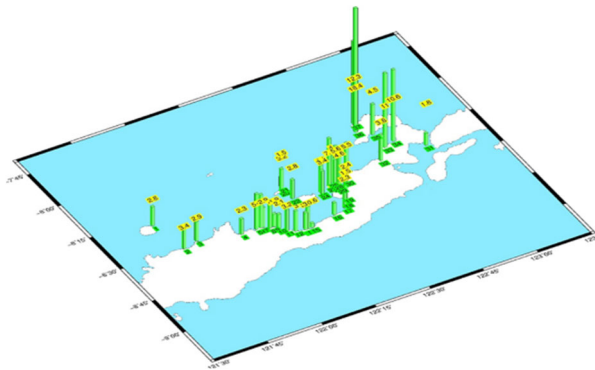


Figure 3. Observed tsunami run-ups plotted with scale bars in a 3D view. The data source is from Hidayat et al. (1995).

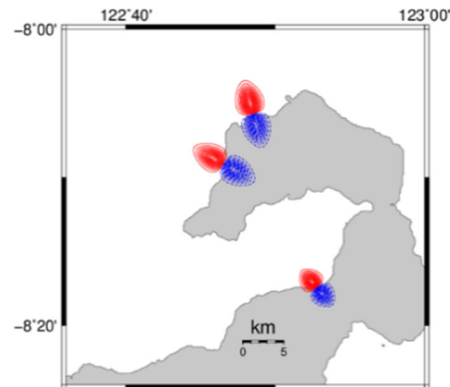


Figure 4. Three landslide models. The red and blue contours with the interval of 1 m indicate the uplift and subsidence predicted from the slump models.

## 3. METHODOLOGY

### 3.1. Tsunami simulation and computational setting

For the tsunami simulations in this study, we used TUNAMI code originally developed by Tohoku University and provided by Yanagisawa (2021). The governing equations are based on the non-linear long wave theory with the spherical coordinate system. For the study area, we confirmed that the recent data for the Flores, BATNAS is more adequate than GEBCO 2020 (GEBCO Compilation Group, 2020). The resolution of GEBCO 2020 is 15 arc-second (<https://www.gebco.net/>). Meanwhile, they are 6 arc-second and 0.27 arc-second for BATNAS and DEMNAS, respectively. This study enhances the tsunami modeling by applying tectonic (earthquake fault) and non-tectonic (landslide) sources. For the tectonic source, we applied two-layer computations by using the two reference fault models. For the non-tectonic sources, we applied three-layer simulations using the fault and three landslide models.

### 3.2. Validation of tsunami simulations results

Validation of the calculations are required in tsunami modeling studies as the confirmation whether the simulation results reproduce the observations. For the validations we refer to the  $K$  and  $\kappa$  numbers (Aida, 1978).  $K$  is a ratio between the measurements and the simulations,  $\kappa$  is a standard deviation indicating the acceptability of the modeling, proposed values of  $0.8 < K < 1.2$  (20% error) and  $\kappa < 1.45$ .

## 4. RESULTS and DISCUSSION

### 4.1. Two-layer computation with fault models

We applied the two-layer nested grids for the numerical tsunami simulations by using two fault models from Imamura et al. (1995) and Pranantyo and Cummins (2019) as shown in Figure 5. Our tsunami modeling results from Imamura et al. (1995) showed that for a tsunami in the densely populated area, Wuring (11) and Maumere (12), the estimated tsunami heights obtained were 1.46 m and 1.44 m, respectively. In Babi Island, as reported by Tsuji et al. (1995), the tsunami wiped away the whole island and the heights we obtained were 2.44 m at Babi North (25) and 1.97 m at Babi East (27). The tsunami in the northern shore of Flores, which approached to Bunga was 12 m, and our obtained result of the model was 2.8 m which was not fitted well with the measurement.

Meanwhile our modelling from Pranantyo and Cummins (2019) for locations of (11) and (12) the estimated tsunami heights obtained were 3.2 m and 3 m, respectively. For locations of 25 and 27, we obtained 4 m and 5.6 m respectively and at Bunga (37) obtained height was 1.03 m. The previous study by Hidayat et al. (1995) also performed tsunami simulations with the fault source inverted from seismic data. For the comparison, we show the bar graph of the simulation results against the observations at 37 outpoints (Figure 6). The two-layer simulation results from the fault models showed that the obtained tsunami run-up heights underestimated the observed values.

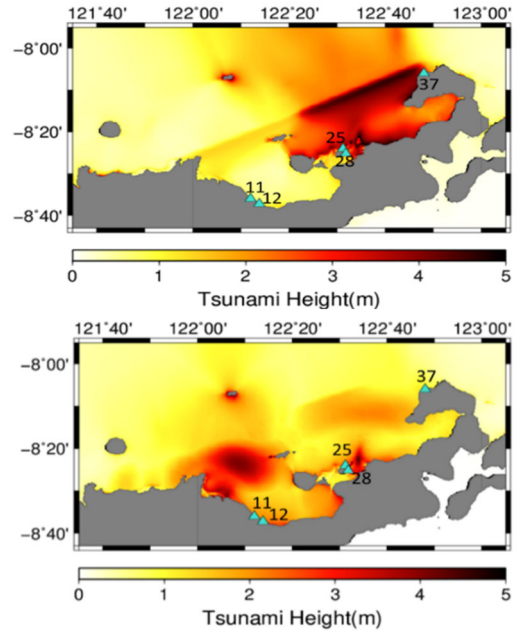


Figure 5. Distribution of calculated maximum tsunami heights from (top) Imamura et al. (1995) and (bottom) Pranantyo and Cummins (2019) fault models.

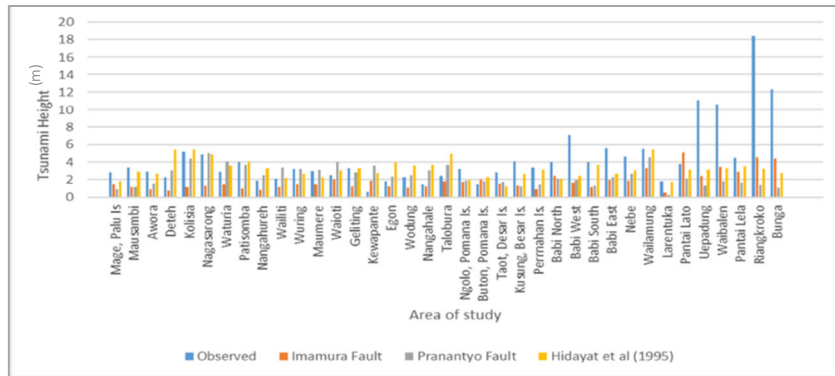


Figure 6. Comparison of tsunami heights for two-layer computations.

### 4.2. Three-layer computation with fault and landslide models

We set the three landslide models located near the coast and the slide directions perpendicular to the coast lines. As the output points for the calculated tsunami waveforms, we selected five locations, Waibalen, Riangkroko, Bunga, Uepadung and Pantai Lela in Layer 3. Uepadung and Pantai Lela are located behind and in front of the landslide model near Waibalen, respectively. For the two-subfault model by Imamura et al. (1995) and three landslide models, we obtained the maximum tsunami heights

of 8.12 m at Waibalen (34) and 11.2 m at Bunga (37). The results slightly underestimated the measured tsunami heights. At Riangkroko (36), the calculated maximum tsunami height was 12 m. We can see the estimated maximum tsunami at all the locations in Figure 7. The other results at location (33) and (35) show the maximum tsunami heights of 5.2 m and 4.5 m.

For the 360-subfault model by Pranantyo and Cummins (2019) and the three landslide models, we obtained the results for locations (34), (36) and (37) of 7.9 m, 8.5 m and 10.4 m, respectively. Figure 8 shows the comparison of the calculated maximum tsunami heights and the observed ones by the field survey and the ones simulated by the previous study (Hidayat et al., 1995). In the Eastern part of Flores, the landslide models had a good certainty to reproduce the tsunami heights. To validate the simulation results, we calculated the  $K$  and  $\kappa$  for the 37 locations. For the first model referred to Imamura et al. (1995) with the landslide models, we obtained  $K = 1.49$  and  $\kappa = 1.39$ , and for the second model of Pranantyo and Cummins (2019) with the landslide models, we obtained  $K = 1.47$  and  $\kappa = 1$ . The validation results showed that the second fault model explained the observation results slightly better than the first simulation.

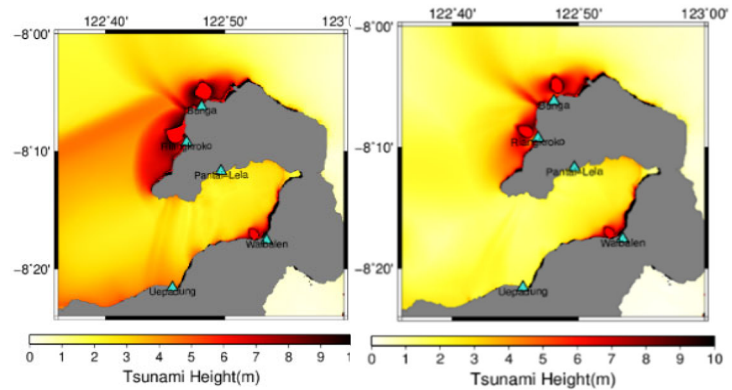


Figure 7. Distribution of calculated maximum tsunami heights from (left) Imamura et al. (1995) and (right) Pranantyo and Cummins (2019) fault models and three landslide models.

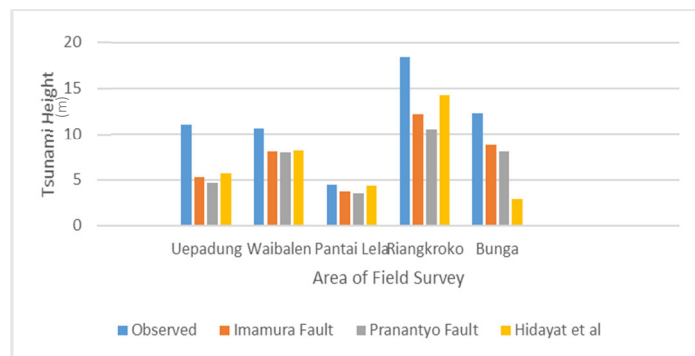


Figure 8. Comparison of tsunami heights for three-layer computations.

#### 4.3. Tsunami inundation simulation for a scenario earthquake

We assumed the fault model refer to Lovholt et al. (2012) and Pusgen (2017) along the Flores back-arc thrust and calculated the seafloor deformation (Figure 9). The maximum uplift was 2.1 m and the maximum subsidence was -0.47 m. This scenario generated huge tsunami and the inundation tsunami in Pota Pota, western Flores (Figure 10). The maximum tsunami run-up of 16 m with the inundation distance of 1,700 m. For this simulation, we did not adopt landslide models, since we need more reference data for potential landslide events. The results can support the creation of a tsunami hazard map. However, to make a tsunami evacuation map for this scenario, further studies are needed

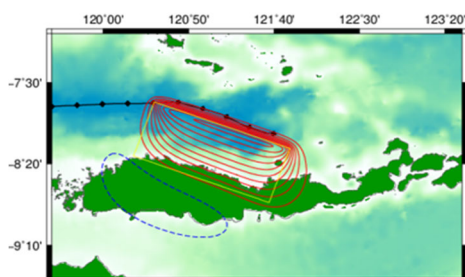


Figure 9. Seafloor deformation from the scenario fault model.

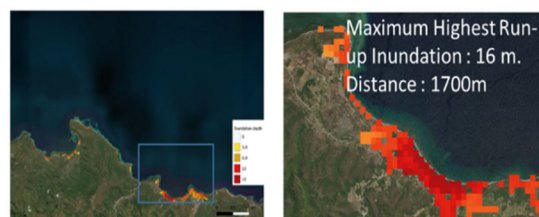


Figure 10. Result of the tsunami inundation simulation from the scenario earthquake for Pota Pota, western Flores.

## 5. CONCLUSIONS

In this study, we modeled the 1992 Flores tsunami using TUNAMI code by adopting two fault models and three landslide models. The two-fault model (Mw 7.8) referred to Imamura et al. (1995) and the 360-subfault model (Mw 7.8) from Pranantyo and Cummins (2019) reproduced higher tsunamis in the eastern part and western part, respectively. This is because of the different position of the large slips on the fault models.

We performed two tsunami inundation simulations with two-layer and three-layer nested grids and evaluated the results with the observed tsunami heights at 37 output points from the field survey measurements Table 3. As the results from the two-layer simulations, the tsunami waveforms and the maximum heights were provided along the coast of Flores. As the results from the three-layer calculation, we involved five locations as the output points in the finest grid (Layer 3). Since we only assumed three locations by using three landslide models, the tsunami heights at the five output points were impacted higher than the two-layer computation.

As the validation of the tsunami simulation results comparing with the tsunami field survey data, we calculated the values of  $K$  and  $\kappa$ . We found that both of the fault models almost explain the tsunami heights by being unified with the three landslide models, especially in the eastern area, although the fitting values of  $K$  and  $\kappa$  still show the slight underestimation.

We designed the size of an earthquake (Mw 8.3) from the reference studies as our scenario to simulate the tsunami propagation. We also performed a tsunami inundation simulation assuming the scenario earthquake to prepare a tsunami hazard map at Pota-Pota in western Flores. If we could find an evidence of landslide potential in future, we are ready for the tsunami modeling using the unified scenario earthquake and landslide models.

## ACKNOWLEDGEMENTS

This research was conducted as the individual study of the training course “Seismology, Earthquake Engineering and Tsunami Disaster Mitigation” by IISEE/BRI, JICA, and GRIPS. I would like to express my sincere gratitude to my supervisor Dr. Yushiro Fujii for his valuable support and experience which helped me to complete my research successfully.

## REFERENCES

- Aida, I., 1978, *Journal of Physics of the Earth*, 26(1), 57-73.  
Daryono, 2011, *Artikel Kebumihan*, Badan Meteorologi Klimatologi dan Geofisika.  
Hamilton, W. B., 1979, *Tectonics of the Indonesian region* (Vol. 1078). US Government Printing Office.  
Hidayat, D., et al., 1995, *Pure and Applied Geophysics*, 144, 537-554.  
Imamura, F., et al., 1995, *Pure and Applied Geophysics*, 144, 555-568.  
Løvholt, F. et al., 2012, *Journal of Geophysical Research: Solid Earth*, 117(B9).  
Pranantyo, I. R., and Cummins, P. R., 2019, *Pure and Applied Geophysics*, 176, 2969-2983.  
Pusgen, 2017, *Peta sumber dan bahaya gempa Indonesia*, Kementerian PUPR  
Tsuji, Y., et al., 1995, *Pure and Applied Geophysics*, 144, 481-524.  
Watts, P., et al., 2005, *Journal of waterway, port, coastal, and ocean engineering*, 131(6), 298-310.  
Yanagisawa, H., 2021, *Lecture Note for Numerical Simulation Tsunami Modelling*.  
Yeh, H., et al., 1993, *Eos, Transactions American Geophysical Union*, 74, 369-373.